Applied Thermal Engineering 246 (2024) 122901

Contents lists available at ScienceDirect

Applied Thermal Engineering

journal homepage: www.elsevier.com/locate/apthermeng

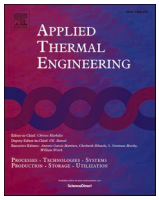

Research Paper

Methanation of syngas from biomass gasification: Small-scale plant design in Aspen Plus

Biagio Ciccone [a,b,*], Fabio Murena [c], Giovanna Ruoppolo [b], Massimo Urciuolo [b], Paola Brachi [b]

[a] Dipartimento di Scienza Applicata e Tecnologia (DISAT), Politecnico di Torino, C.so Duca degli Abruzzi 24-10129, Torino, Italy
[b] Istituto di Scienze e Tecnologie per l'Energia e la Mobilità Sostenibili, Consiglio Nazionale delle Ricerche, P. le V. Tecchio, 80-80125 Napoli, Italy
[c] Dipartimento di Ingegneria Chimica, dei Materiali e della Produzione Industriale (DICMaPI) Università degli Studi di Napoli Federico II, P.le V. Tecchio, 80-80125 Napoli, Italy

ARTICLE INFO

Keywords:
Syngas methanation
Nitrogen dilution
Plant design
Aspen Plus
Sensitivity

ABSTRACT

The objective of this study is to investigate the upgrading of low-quality nitrogen-diluted syngas derived from biomass air gasification processes into a methane-rich gas stream. Both the thermodynamic and the kinetic aspects are addressed in the paper. Using the Aspen Plus software, a thermodynamic analysis was conducted; then, different plant designs are simulated and compared, including reactor sizing and performance. The results demonstrate that the upgrading of diluted syngas poses challenges which limit its application to small-scale decentralized systems. It was found that a system comprising of four adiabatic fixed-bed reactors, intercooling, and efficient water removal achieves a favorable balance between performance and cost. Operating the system at a pressure of 5 bar is deemed adequate as it reduces the required catalyst mass and prevents solid carbon deposition. Notably, this configuration achieved good results, including a 99.4 % CO conversion, 89.3 % CO_2 conversion, and 95.6 % CH_4 yield. The final methane molar content reached 26.4 %, with a calorific value of 8.62 MJ/Nm^3(STP).

1. Introduction

Fossil fuels, despite driving industrial progress with their high energy-to-volume ratio, cost-effectiveness, and ease of storage, are deemed unsustainable due to finite natural gas reserves [1], long-term environmental consequences [2], and the flawed notion that they can meet growing energy demands [3]. Unfortunately, renewable alternatives like solar and wind power face efficiency fluctuations, posing challenges in fully replacing fossil fuels.

In recent years, there has been a burgeoning interest in biomass-derived energy, with both wet and dry biomass emerging as promising starting materials for energy production. Among the thermochemical processes for biomass conversion, gasification stands out for its capacity to yield versatile syngas, crucial for energy generation and chemical synthesis [4]. However, challenges in large-scale centralized gasification facilities, stemming from low bulk densities of most biomasses, have prompted investments in small-scale plants, as seen in initiatives by European countries like Germany and Italy [5]. Small-scale biomass plants hold potential for enhancing energy supply in remote locations [6].

Catalytic methanation emerges as a practical method to enhance syngas quality from biomass gasification. This process involves the hydrogenation of carbon oxides, generating methane gas through specific catalysts. The exothermic nature of CO and CO_2 methanation necessitates careful heat management to prevent catalyst damage [7,8].

Synthetic natural gas (SNG), with its high conversion efficiency and compatibility with natural gas infrastructure, presents a promising alternative to traditional fossil fuels. The well-established natural gas transportation network and end-use technologies further position SNG as a viable option for utilities.

In this context, methanation reactor modeling is a crucial aspect that can be approached at various levels, ranging from zero to three dimensions. One-dimensional (1D) models are commonly utilized for identifying qualitative trends and optimizing operating parameters, as they provide results closely aligned with those derived from more computationally intensive two-dimensional (2D) models [8]. The preference for 1D models in overall plant feasibility studies and preliminary reactor design is due to their computational efficiency, while three-dimensional (3D) models become essential for comprehensive design and optimization purposes. Aspen Plus is frequently employed for modeling methanation reactors in the context of synthetic natural gas

* Corresponding author at: Dipartimento di Scienza Applicata e Tecnologia (DISAT), Politecnico di Torino, C.so Duca degli Abruzzi 24-10129, Torino, Italy.
E-mail address: biagio.ciccone@stems.cnr.it (B. Ciccone).

https://doi.org/10.1016/j.applthermaleng.2024.122901
Received 11 September 2023; Received in revised form 6 March 2024; Accepted 7 March 2024
Available online 9 March 2024

Nomenclature

List of symbols

$\mathfrak{D}$	Mean gas diffusivity [m^2/s]
D_p	Particle diameter [m]
D_t	Reactor diameter [m]
ε	Bed void fraction [-]
ϕ	Effectiveness factor for intra-particle transport limitation [-]
η_C	Carbon yield [-]
η_{CH4}	Methane yield [-]
K_1	Equilibrium constant for reaction 1 [bar^2]
K_2	Equilibrium constant for reaction 2 [-]
K_3	Equilibrium constant for reaction 3 [bar^2]
K_{CH4}	Adsorption constant of CH_4 [bar^{-1}]
K_{CO}	Adsorption constant of CO [bar^{-1}]
K_{H2}	Adsorption constant of H_2 [bar^{-1}]
k_i	Kinetic constant of reaction *I* [$kmol/kg_{cat}$ h]
L	Catalyst bed length [m]
L_{eq}	Minimum bed length to reach equilibrium [m]
μ_f	Viscosity of gas mixture [Pa s]
N	Mole flowrate [kmol/h]
P	Pressure [bar] or [Pa]
Q_m	Gas flow rate [m^3/s]
R	Mole-based recycle ratio [-]
ρ_f	Density of gas mixture [kg/m^3]
T	Temperature [K] or [°C]
U_g	Superficial gas velocity [m/s]
x_{CO}	CO conversion [-]
x_{CO2}	CO_2 conversion [-]
z	Reactor axial coordinate [m]

Abbreviation

C	Solid carbon
CH_4	Methane
CHP	Combined heat and power
CO	Carbon monoxide
CO_2	Carbon dioxide
FBR	Fixed bed reactor
H_2	Hydrogen
H_2O	Water
HHV	Higher heating value
LHV	Lower heating value
N_2	Nitrogen
Pe	Peclet number
PR	Peng Robinson
RFBR	Recycle fixed bed reactor
SNG	Synthetic natural gas

(SNG) production facilities. The ongoing advancements in methanation technology and modeling underscore the continuous efforts of researchers in this domain.

Er-rbib and Bouallou [9] proposed a three-stage catalytic fixed bed methanation system for storing renewable energy as methane using syngas and CO methanation, making clear how renewable energy sources can be integrated in the methanation process. Matthischke et al. [10] compared adiabatic and cooled fixed-bed reactors, finding that product recirculation in adiabatic reactors cooled the temperature and improved methane production. Adiabatic reactors were noted to be more versatile, while cooled reactors had a shorter start-up time.

Chein et al. [11] investigated the effects of operating conditions and syngas composition on reactor performance. They demonstrated that the syngas inlet temperature significantly influenced CO conversion, favoring isothermal operation over adiabatic, in which hot-spots can arise. The authors underline that syngas produced from coal or biomass gasification as a low H_2/CO ratio, making it necessary to adjust the hydrogen content. Kao et al. [12] explored strategies to improve temperature control in fixed-bed methanation reactors, including the employment of cooled reactors, the recycling of the effluent gas, and water addition to the reacting mixture. They concluded that both the use recycle reactors and steam addition can mitigate the temperature rise in the methanation reactor.

The existing body of literature concentrates on the enhancement of syngas derived from steam and/or oxygen gasification, characterized by a typically high H_2/CO ratio [13]. This optimized syngas can become suitable for grid injection, after specific standards are met [14]. In contrast, poor attention has been directed towards exploring the potential of diluted syngas resulting from air gasification—a cost-effective and state-of-the-art technology [15]. Syngas produced through air gasification is heavily diluted with nitrogen [16], posing challenges concerning compliance with standard requirements for injection into the natural gas grid and for the direct utilization for CHP systems. This includes issues such as nitrogen-induced reductions in the Wobbe Index and heating values of the Synthetic Natural Gas (SNG).

However, a combined system integrating air gasification and catalytic methanation holds promise, particularly in regions with surplus renewable energy [15]. This surplus energy can be utilized for hydrogen production through electrolysis, subsequently stored in the stable form of chemical bonds within SNG. Methane, being more manageable than hydrogen and presenting fewer safety concerns during storage and distribution, emerges as an advantageous energy carrier.

The current study aims to explore the theoretical feasibility of upgrading low-quality syngas derived from biomass air gasification into a methane-rich gas stream through catalytic methanation. This exploration is conducted from both thermodynamic and kinetic perspectives. The Aspen Plus software package serves as a valuable tool for simulating and comparing various plant configurations, allowing an investigation into the impact of different operating conditions on process performance.

2. Materials and methods

The Aspen Plus software was used to model the conversion of syngas to bio-methane, with the syngas composition retrieved from an experimental study where the biomass gasification with air was performed using a small-scale commercial plant [16]. The focus of the work [16] was to produce syngas for a spark-ignition internal combustion engine using a fixed-bed downdraft gasifier in a micro-CHP plant.

The dry-basis composition of the syngas adopted in all subsequent simulations is specified in Table 1, while the mass flow rate is 58.32 kg h^{-1} and the temperature is 47.6 °C. The dry-basis composition of the syngas was considered as the starting point for the methanation process because the syngas undergoes some cleaning steps to remove ash, char and impurities (tars) and is completely cooled and dried in the process [16]. Nevertheless, the syngas temperature is set to 25 °C in the

Table 1
Syngas composition adopted in the simulation [16].

Component	[v/v %] d.b.
CO	15.9
CO_2	9.16
CH_4	1.24
H_2	12.2
N_2	61.5

following sections, as it does not change the conclusions.

Fig. 1 shows a schematic representation of the flow of the present work. Initially, a thermodynamic analysis is undertaken to identify optimal operating conditions that maximize methane yield while minimizing char production. The insights gained from this analysis serve as a foundation for subsequent kinetic modelling. A literature-based kinetic model is employed to explore various system configurations, ranging from a single-stage adiabatic fixed-bed methanation (S1) to more complex multi-stage recycle methanation systems with inter-cooling (S4).

Finally, a parameter-by-parameter sensitivity study is conducted to pinpoint suitable operating conditions for an optimized small-scale system. This systematic approach allows for a nuanced understanding of the complex interplay between thermodynamics, kinetics, and system configurations, facilitating the identification of conditions that enhance methane production efficiency while mitigating undesired byproducts such as char.

2.1. Thermodynamic analysis

The simulations were performed using the Aspen Plus software and the key aspects pertaining to the specified compounds, property method, and employed blocks are presented as follows:

- In addition to the compounds found in the feed stream, namely CO, CO_2, CH_4, H_2, and N_2, additional components included in the simulation are water and pure solid carbon. The presence of pure solid carbon may arise from the simple cracking of methane and/or through the Boudouard reaction occurring on the catalyst's surface [8,17]
- For the description of gases encompassing diverse temperature and pressure conditions, the Peng-Robinson (PR) equation of state was selected because it is well-suited for non-polar or mildly polar gas mixtures containing light gases, especially at high temperature and pressure ranges [18]. All binary interaction parameters were directly sourced from the Aspen Plus library.
- To facilitate the computations, the RGIBBS block was employed, as illustrated in Fig. 2, which shows a schematic representation of the Aspen Plus flowsheet for the thermodynamic analysis. This block operates under the fact that the change in Gibbs free energy (dG) is zero when equilibrium conditions are achieved. Irrespective of the reactions involved, the RGIBBS model establishes the composition of the output mixture corresponding to the minimum of the Gibbs free energy with respect to temperature, pressure, and composition.

The concentrations of water and solid carbon were set to zero at the reactor inlet. This zero-dimensional (0D) approach allowed for a rapid and cost-effective estimation of the system's composition at equilibrium, thereby enabling a preliminary investigation into the practical and technological feasibility of the syngas methanation process. When the amount of the available hydrogen is insufficient to ensure complete conversion of carbon oxides to methane, supplementary hydrogen (EXTRA-H_2 stream in Fig. 2) must be provided, e.g., from water electrolysis driven by surplus renewable energy.

2.1.1. Case I: No extra hydrogen provided

A sensitivity study allowed to investigate the trend of CO conversion, CO_2 conversion, methane yield and solid carbon yield, when the reactor temperature and pressure are changed. In this section, there is no hydrogen addition to the system. Using the Aspen Plus sensitivity tool, the temperature was varied within the range of 100 to 1000 °C with a step size of 10 °C and the pressure was set at three distinct levels: 1, 15 or 30 atm. After properly setting the molar flow rates and output compositions in the "Tabulate" section, the following values were defined as dependent variables to be evaluated: the molar fractions of all the species in the outflow stream at equilibrium, the CO conversion (x_{CO}), the CO_2 conversion (x_{CO_2}), the methane yield (η_{CH_4}), the solid carbon yield (η_C), the lower heating value (LHV) and higher heating value (HHV) of the output mixture.

2.1.2. Case II: Extra hydrogen provided

In this second scenario, the sensitivity analysis was conducted with a different approach. The pressure value was kept constant at the reference pressure of 1 bar throughout the study and the temperature was varied between 100 and 1000 °C as the independent variable. Moreover, the mass flow rate of the hydrogen added was introduced as a parameter at three specific levels:

1. 0 kg h^{-1}: Corresponding to the case where no additional hydrogen is supplied (cfr. Case I)
2. Stoichiometric conditions (3.24 kg h^{-1}): the hydrogen mass flow rate was adjusted to meet the stoichiometric requirements for complete conversion of CO and CO_2 to methane.
3. 15 % excess (3.73 kg h^{-1}): an arbitrary excess amount of hydrogen was provided.

The same variables of Case I were considered for this section as well. This approach allowed for a thorough examination of how the selected variables respond to changes in temperature and different hydrogen mass flow rate conditions, under a constant pressure value of 1 bar. When additional hydrogen is mixed to the syngas, the overall composition and the $H_2/CO/CO_2$ ratios will change accordingly. The composition of the syngas with stoichiometric and excess hydrogen is reported in Table 2, while the definitions of all the parameters used in the results section are provided in Table 3.

2.2. Kinetic model

The model presented by Xu & Froment [19] was used in this work since it is regarded as one of the most trustworthy and complete currently accessible.

In Aspen Plus, the kinetic parameters need to be rearranged to adhere to specific format requirements. Specifically, these parameters should be declared by providing coefficients for temperature polynomials as follows (Eq. (1)):

$$\ln(k) = A + \frac{B}{T} + C\ln(T) + DT \tag{1}$$

In Eq. (1), k stands for the kinetic constant, and T denotes the temperature in Kelvin. The coefficients A, B, C, and D must be specified to accurately describe the temperature dependence of the kinetic factor.

However, it is important to note that only the kinetic factor of the driving force should be declared in terms of its activation energy and pre-exponential factor. On the other hand, the rate and adsorption constants are defined separately in Table 4, and their temperature

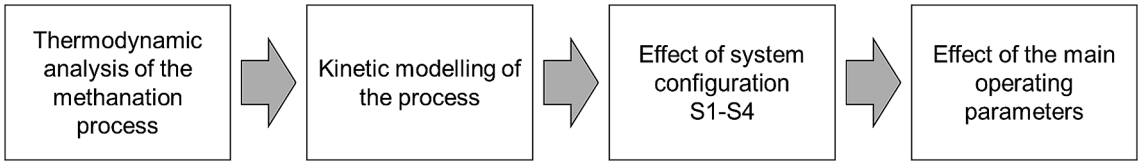

Fig. 1. Flow of the present work.

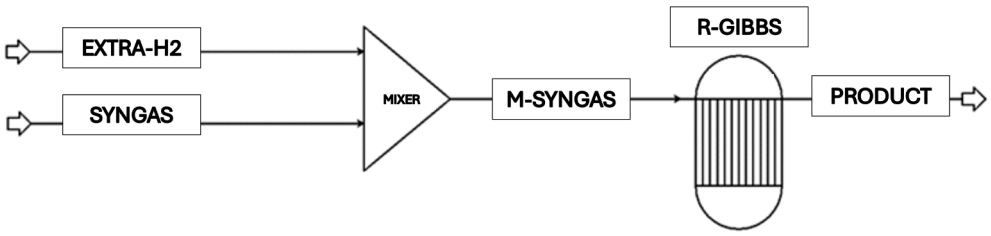

Fig. 2. Equilibrium simulation flowsheet.

Table 2
Syngas composition [mol/mol %] with stoichiometric and excess hydrogen.

	Stoichiometric H_2	Excess H_2
CO	9.24	8.69
CO_2	5.32	5.00
CH_4	0.72	0.67
H_2	48.99	52.00
N_2	35.73	33.62

dependence is described using the Arrhenius and Van't Hoff equations, respectively.

Aspen Plus was used to calculate the chemical equilibrium constants (i.e., K_1, K_2 and K_3 in Table 4) for the three reactions involved. A simulation was built up using the REQUIL block, and a sensitivity analysis was performed to compute the equilibrium constant at different values of the reactor operating temperature. The resulting numerical data was then linearized.

2.3. Model validation

To validate the Aspen kinetic model, data from real industrial plants were utilized. Specifically, reference was made to the work of Khorsand et al. [20], who conducted a modeling study on the methanation unit of an ammonia synthesis plant. The findings of their simulation were compared to actual industry data, providing a way to validate the Aspen kinetic model.

For this validation process, all the operating parameters were adopted from the industrial data reported by Khorsand et al. [20]. These parameters included input molar flows, temperature and pressure conditions, as well as reactor dimensions and catalyst properties. A comparison between the simulated results and the corresponding industry data allowed to assess the accuracy and reliability of the model.

2.4. Reactor sizing and design procedure

Methanation reactors are modelled using Aspen Block RPLUG block, which is designed to represent perfect plug-flow reactors. Since no radial concentration and temperature profiles are expected in normal operating conditions, namely when the reactor is working properly and a well-developed fluid-dynamic regime is established, due to the absence of a cooling medium, the RPLUG one-dimensional model is suitable for describing adiabatic fixed-bed reactors [21]. In this modelling approach, axial mass and heat transfer are also assumed to be negligible, and all the process is at steady state. The Ergun equation is selected to estimate the pressure drops in the catalytic bed. The Ergun momentum balance equation is included in the Aspen Plus RPLUG block, and can be written as follows (Eq. (2)):

$$\frac{dP}{dz} = \frac{150(1-\varepsilon)^2 \phi U_g}{\varepsilon^3 D_p^2} + \frac{1.75(1-\varepsilon) U_g \rho}{\varepsilon^3 D_p} \quad (2)$$

where P is the pressure [Pa], z is the reactor axial coordinate [m], U_g is the fluid velocity [m/s], ϕ is an effectiveness factor for intra-particle transport limitation [-], D_p is the particle diameter [m], ρ is the catalyst density [kg/m^3] and ε is the catalyst bed void fraction.

The kinetic modeling of solid carbon formation was not included in the simulations and the absence of solid carbon formation was ensured only by a thermodynamic approach.

The decision to employ a single-tube configuration for simulating methanation reactors is motivated by a specific focus on fixed-bed adiabatic reactors designed for small-scale applications in this study.

Table 4
Kinetic parameters and corresponding Aspen coefficient (adapted from [19]).

Parameter	Equation	Aspen coefficients
k_1	$k_1 = 4.22510^{15}\exp\left(-\frac{240.1}{RT}\right)$	$\begin{cases} k_1 = 4.225\ 10^{15} \\ E_1 = 240.1\ KJ/mol \end{cases}$
k_2	$k_2 = 1.95510^{6}\exp\left(-\frac{67.13}{RT}\right)$	$\begin{cases} k_2 = 1.955\ 10^{6} \\ E_2 = 67.13\ KJ/mol \end{cases}$
k_3	$k_3 = 1.02010^{15}\exp\left(-\frac{243.9}{RT}\right)$	$\begin{cases} k_3 = 1.020\ 10^{15} \\ E_3 = 243.9\ KJ/mol \end{cases}$
K_{CO}	$K_{CO} = 8.2310^{-5}\exp\left(\frac{70.65}{RT}\right)$	$\begin{cases} A_{CO} = -9.40 \\ B_{CO} = 8497.2 \end{cases}$
K_{H_2}	$K_{H_2} = 6.1210^{-9}\exp\left(\frac{82.90}{RT}\right)$	$\begin{cases} A_{H_2} = -18.90 \\ B_{H_2} = 9971.1 \end{cases}$
K_{CH_4}	$K_{CH_4} = 6.6510^{-4}\exp\left(\frac{38.28}{RT}\right)$	$\begin{cases} A_{CH_4} = -7.32 \\ B_{CH_4} = 4604.3 \end{cases}$
K_{H_2O}	$K_{H_2O} = 1.7710^{5}\exp\left(-\frac{88.68}{RT}\right)$	$\begin{cases} A_{H_2O} = 12.08 \\ B_{H_2O} = -10666.3 \end{cases}$
K_1	$K_1 = \exp\left(29.206 - \frac{26032}{T}\right)$	$\begin{cases} A_{R1} = 29.206 \\ B_{R1} = -26032 \end{cases}$
K_2	$K_2 = \exp\left(-4.342 + \frac{4686.7}{T}\right)$	$\begin{cases} A_{R2} = -4.342 \\ B_{R2} = 4686.7 \end{cases}$
K_3	$K_3 = \exp\left(24.719 - \frac{21233}{T}\right)$	$\begin{cases} A_{R3} = 24.719 \\ B_{R3} = -21233 \end{cases}$

Table 3
Main parameters evaluated in the thermodynamic analysis.

Parameter	Definition	Notes
CO conversion	$X_{CO}(\%) = 100\frac{N_{CO\,in} - N_{CO\,out}}{N_{CO\,in}}$	'N' denotes mole flow rate
CO_2 conversion	$X_{CO_2}(\%) = 100\frac{N_{CO_2\,in} - N_{CO_2\,out}}{N_{CO2\,in}}$	'N' denotes mole flow rate
CH_4 yield	$\eta_{CH_4}(\%) = 100\frac{N_{CH_{4_{out}}}}{\sum NC_i N_{iin}}$	Subscript i denotes all carbon-containing species (CO, CO_2, C, and CH_4), while NC_i denotes the number of carbon atoms in species i.
Carbon yield	$\eta_C(\%) = 100\frac{N_{C_{out}}}{\sum NC_i N_{iin}}$	Subscript i denotes all carbon-containing species (CO, CO_2, C, and CH_4), while NC_i denotes the number of carbon atoms in species i.

Unlike multi-tube reactors, which are typically employed for enhanced productivity and utilize a cooling medium to achieve a polytropic temperature profile, the choice of a single-tube design aligns with the targeted context of small-scale methanation. The catalyst parameters used in the simulations were provided by Matthischke et al. [10]. These parameters pertain to a commercial Ni/Al_2O_3 catalyst with sphere-shaped particles, as outlined in Table 5.

Reactor sizing employed the Aspen Plus sensitivity tool, adhering to theoretical and plant engineering constraints. The RPLUG model, requiring catalyst bed length (L) and reactor diameter (Dt), allowed for varied L/Dt ratios to achieve consistent catalyst mass and CO/CO_2 conversion. To constrain system parameters, empirical restrictions from Woods [22] were applied, aligning theoretical and practical considerations for a robust sizing methodology. Among these, one can mention:

- The recommended catalyst particle size should be in the range of 1–5 mm.
- The mean residence time within the reactor should be less than 1 s.
- Pressure drops should be limited to less than 10 %.
- Turbulent flow is necessary to have proper plug-flow, therefore the particle Reynolds number, defined as (Eq. (3)):

$$Re_p = \frac{\rho_f D_p 4 Q_m}{\pi D_T^2 (1-\varepsilon)\mu_f} \tag{3}$$

should be greater than 100 [23].

- It is preferable to have an axial Peclet number (defined as $Pe = U_g D_t/\mathfrak{D}$, where U_g is the mean velocity, D_t is the tube diameter and $\mathfrak{D}$ is the mean diffusivity) greater than two to ensure optimum gas distribution and minimal back mixing. The Peclet number can be estimated using a rough correlation provided by Wen (in [24]).

As mentioned before, the outlet temperature should be carefully managed due to catalyst deactivation [8]. In most models, outlet temperatures ranging from 500 to 650 °C are employed [11,12,9]. To ensure that equilibrium conversion is achieved, the reactor length is adjusted in Eq. (4):

$$L = L_{eq}(1+\vartheta) \tag{4}$$

where ϑ is a safety factor ranging from 0.3 to 0.4, and L_{eq} is the minimum bed length necessary to reach equilibrium conditions, i.e., the point where the temperature profile hits a plateau.

2.5. Plant design configurations

This section entails with the description of the methanation systems studied in this paper. A path of growing complexity was followed, starting from the simple single stage adiabatic methanation, to more complex systems including multi-stage, inter-cooled systems.

Single stage methanation (System 1-S1)

Fig. 3 demonstrates the configuration of the process using a single fixed-bed adiabatic reactor:

Raw syngas from biomass air-gasification is combined with additional hydrogen to achieve the stoichiometric ratio ($CO/CO_2/H_2 = 1/1/7$). The gas mixture is then heated up at constant pressure to 330 °C before entering the methanation reactor. Inlet temperatures below 250 °C are normally avoided due to limited methanation activity [8]. Moreover, at low temperatures the formation of nickel tetracarbonyl with the CO vapor–solid reaction can occur, resulting in catalyst deactivation owing to nickel loss [17]. This process may be described as follows (Eq. (5)):

$$Ni_{(s)} + 4CO_{(g)} \leftrightarrow Ni(CO)_{4(g)} \tag{5}$$

The plant pressure was set to 2 bar across the unit. As the design stage does not consider the plant's piping network, pressure drop calculations are performed only for the reactors. Before entering the methanation unit, the syngas must undergo proper cleaning and cooling. Therefore, the inlet temperature is set to be at ambient conditions.

Fixed-bed recycle reactor (System 2- S2)

The scheme of *System 1* proves technically unfeasible due to the high outlet temperature, which poses the risk of thermal runaway and catalyst deactivation. To address these challenges, recycling a portion of the product gas back to the reactor's inlet can offer several benefits [10,12]:

1. An optimized recycle ratio can extend the "reactive volume" within the reactor. The reactive volume refers to the portion of the reactor length where a non-zero temperature differential is observed. By achieving an ideal recycling ratio, the reactive volume can occupy the entire reactor volume, leading to a more effective utilization of the catalyst bed. Additionally, equilibrium conditions can be precisely achieved at the reactor outlet.
2. Diluting the feed by mixing it with the recycle stream reduces the overall reaction rate and subsequently lowers the exit temperature. The recycle ratio can serve as a controlled variable in temperature control systems, allowing for enhanced temperature management and preventing issues related to excessive overheating.
3. The decrease in the average temperature within the reactor results in an elevation of the equilibrium degree of conversion of CO and CO_2, leading to higher concentrations of methane in the effluent stream. This is a consequence of the more favourable thermodynamic conditions prevailing at lower temperatures, which facilitate increased methane production (cfr. Fig. 8a and Fig. 9a).

Despite the benefits of improved reactor performance, it is essential to acknowledge that the implementation of recycling reactors comes with additional costs. Notably, the expenses are primarily associated with gas compression. The compressor, though not explicitly shown in the following flowsheets, plays a crucial role in bringing the recycled product back to the original feed pressure. This equipment is expensive, demanding continuous maintenance and consuming power to function effectively.

In the present study, pressure drops are not considered for coolers, piping, and mixers; hence, the compressor is not depicted in the one-stage recycling reactor scheme (Fig. 4):

In this configuration, hot syngas is combined with recycled gaseous products and fed into the reactor. Thanks to an adequate recycling ratio, the exit stream approaches 550 °C and must be cooled before being partially recycled. To simplify the process, it was decided to cool the reactor exit stream to 330 °C. Notably, this temperature matches the temperature of the PRE-MIX stream. Adopting this approach has the advantage of having a consistent and fixed temperature at the reactor's inlet, independent of the recycle stream's temperature.

Series of fixed-bed reactors (System 3-S3)

Since it is essential for SNG to be predominantly composed of methane, additional stages are required to obtain significant CO_2 conversion. While CO can be easily converted in a few steps, CO_2 is far less reactive when nickel catalysts are used [25]. This difference in reactivity can be attributed to the kinetic competition between carbon oxides for the active metal sites on the catalyst surface. Studies have claimed that CO_2 transformation does not occur until most of the CO has reacted [25,26]. Fig. S1 in the Supplementary Material illustrates the multi-

Table 5
Catalyst parameters adopted in the Aspen simulation (ref. [10]).

Catalyst parameters used in the simulation		
Diameter [mm]	3	Typical for fixed bed
Bed porosity [-]	0.39	Typical for spheres
Particle density [kg/m^3]	1475	Reference to Meth134 catalyst
Bulk density [kg/m^3]	900	Calculated

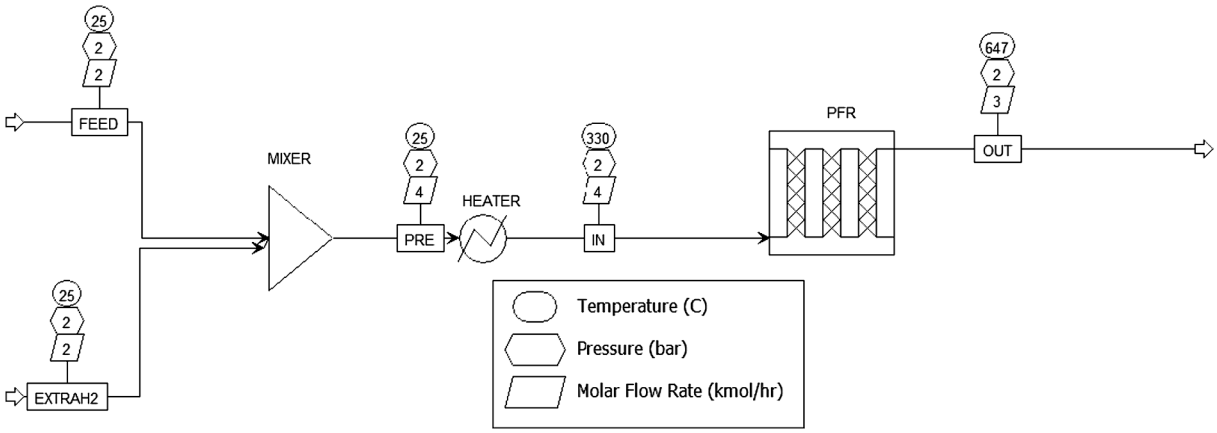

Fig. 3. Single stage methanation system.

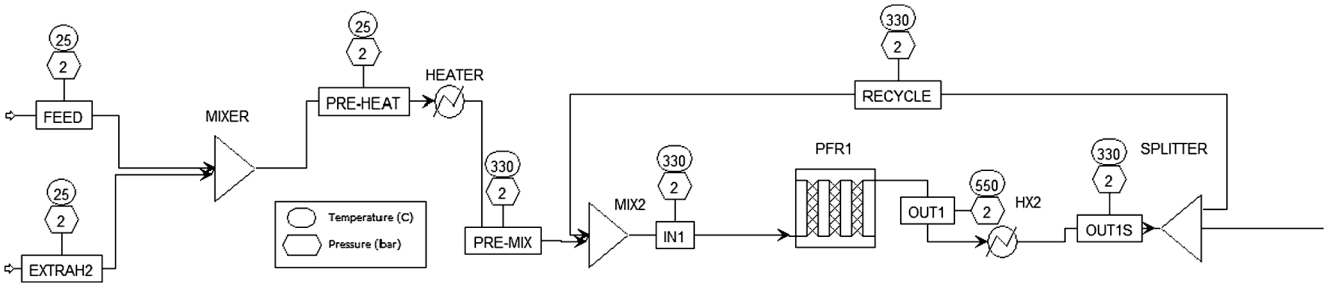

Fig. 4. Single stage recycle reactor.

stage process.

Following the recycling loop, a fraction of the exit stream from the first reactor is directed to a series of four fixed-bed reactors with intermediate cooling sections, where the temperature is reduced to 330 °C at the entrance of all four reactors. The cooling temperature is carefully chosen to strike a balance between achieving high thermodynamic conversion and ensuring the catalyst remains active. The catalyst activation temperature is largely dependent on the specific catalyst employed. For most commercial Ni/Al_2O_3 catalysts, discrete activity is observed when the temperature exceeds 250 °C. It is important to note that while having the same inlet temperature for all reactors is not a strict requirement, it is a common practice in SNG plant simulations [12].

Inter-cooling & water condensation (System 4-S4)

According to the thermodynamic study, the removal of water can improve the performance of the system by shifting the thermodynamic equilibrium towards the products, allowing for increased methane generation. Water removal is accomplished with a condenser. Aspen Plus provides the Flash2 Block, which can be used to simulate liquid–vapor thermodynamic equilibrium [18]. Fig. S2 shows the integration of condensers in the methanation plant.

In this methanation plant configuration, water condensation is carried out after each reactor, and the condensed water is collected. All condensers within the plant operate at the same temperature and pressure, specifically 30 °C and 2 bar, respectively. The chosen temperature is set to ensure that at least 90 % of the incoming water is effectively condensed through the unit, while the pressure is maintained at the plant's operating pressure.

To achieve the cooling required for the streams entering the condensers, a cooling medium is employed. The Flash2 block allows the association of a utility stream directly within the block. Given the presence of numerous high-enthalpy streams departing from the reactors, the plant has an abundance of available heat sources, making it straightforward to utilize excess enthalpy to heat up the output streams from the condensers. This approach simplifies the design process and ensures the effective integration of cooling within the system. This study prioritizes offering an overview of methanation processes for diluted syngas; therefore, a simplified shortcut design for heat exchangers suffices, with no pursuit of in-depth analysis or rigorous design, as these aspects diverge from the study's primary focus. Pressure drops in condensers and exchangers are also neglected here.

2.6. Sensitivity analysis and optimization

The flowsheet presented in Fig. S2 cannot be considered technically or economically favourable due to its complexity, as it includes five reactors and three water removal units. To optimize the plant layout and reduce costs, a parameter-by-parameter sensitivity analysis was conducted to determine the impact of plant parameters, and thus to identify the most advantageous combination. While this procedure is not intended to be a comprehensive economic study, it offers a semi-quantitative assessment of satisfactory conditions. Indeed, the plant costs are represented by the catalyst mass required to achieve thermodynamic equilibrium at the reactor outlet.

The scheme (Fig. 5) below outlines the phases that lead to the best design.

2.6.1. Effect of plant pressure

The influence of plant pressure on the overall system performance was examined. The flowsheet shown in Fig. S2 served as the initial setup for further simulations. Throughout these simulations, all major parameters, such as reactor inlet temperature, recycling reactor exit temperature, and the number of water removal units, remained unchanged.

The impact of pressures set at 2, 5 and 8 bar was investigated. For each pressure condition, the reactor designs were repeated, and the catalyst bed lengths were adjusted to achieve equilibrium. It should be noted that the recycling flow rate required to keep a 550 °C outlet temperature varies with pressure according to Le Châtelier's principle.

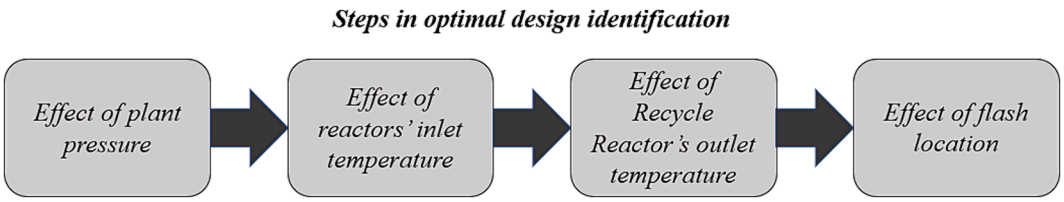

Fig. 5. Optimal design identification procedure followed in this study.

2.6.2. Effect of reactor inlet temperature

In the updated flowsheet, the pressure has been adjusted and set to the satisfactory value determined in the previous analysis (cf. Section 3.4.1: Effect of plant pressure). With the pressure fixed at the optimal level, the inlet temperatures of all reactors were subsequently adjusted to assess their impact on the overall system performance. Specifically, two different inlet temperature scenarios were considered: 330 °C and 350 °C.

2.6.3. Effect of recycle Reactor's outlet temperature (i.e., recycle ratio)

It was deemed intriguing to investigate whether reducing the output temperature of the recycling reactor (RFBR) – effectively increasing the recycle flow rate – would be advantageous in terms of reducing overall expenses and improving performance. For this simulation, the pressure was set to the value determined in Section 3.4.1, and the inlet temperatures of all reactors were set at 330 °C. The only parameter changed was the outlet temperature of the recycling reactor (RFBR), which was changed from the initial 550 °C to the reduced temperature of 500 °C.

2.6.4. Effect of condenser location

The final analysis conducted in the study aimed to explore the possibility of minimizing the number of condensers required in the methanation plant and to identify the ideal location where maximum conversion of CO and CO_2 could be achieved.

3. Results and discussion

3.1. Thermodynamic analysis results

The findings of the thermodynamic analysis are provided and discussed in this paragraph. In the interest of brevity, the results of the thermodynamic analysis in the case of a lack of hydrogen (Case I) have been omitted from the main text because they are of limited interest for the following considerations and are available in the Supplementary Material (cfr. Figg. S3-S5). According to the results, the methanation process is completely unfeasible unless additional hydrogen is added to the syngas to meet at least the stoichiometric ratio.

The plot of Fig. 6 illustrates the thermodynamic equilibrium compositions when hydrogen is added to the raw syngas to meet stoichiometric conditions at 1 bar. In this scenario, carbon monoxide is completely converted at low temperatures, leading to the main reaction products (water and methane). However, carbon dioxide is only partially converted, as evident from Fig. 6. It should be noted that hydrogen addition results in a substantial reduction of carbon deposition. Fig. 6 clearly depicts that a pure solid carbon phase is present only within a limited temperature range, specifically between 450 and 660 °C. This specific trend of the solid carbon production is observed in the literature [27]. This can be explained by the fact that reactions producing char (namely, CH_4 cracking and the Boudouard equilibrium) are encouraged compared to the methanation reactions in the temperature range 450–650 °C [27].

It can be demonstrated that the presence of high N_2 dilution deeply influences the global Gibbs free energy of the system, thus leading to the production of solid carbon in a specific temperature range, which becomes wider with increasing dilution. Furthermore, the methane content in the product is notably higher compared to the case where there is

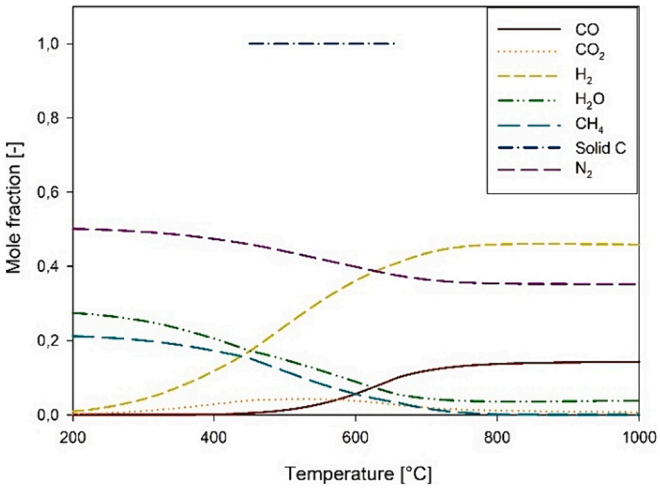

Fig. 6. Equilibrium composition of the syngas with stoichiometric H_2 at 1 bar.

a lack of hydrogen in the syngas. In the presence of hydrogen, the methane content reaches a maximum of 22 % by volume. Notably, the methane mole fraction is particularly higher at low temperatures.

Fig. 7a and Fig. 8a present the trends of the degree of conversion of CO and CO_2 with temperature when stoichiometric hydrogen is present in the reacting syngas, considering different operating pressures. The results show that at low temperatures and high pressures, there is a significant conversion of both carbon oxides. Notably, in the temperature range of 500 to 700 °C, the conversion of CO is generally higher than the conversion of CO_2. However, as the temperature continues to rise, reaching around 650 °C, the trends shift. CO_2 conversion starts to increase rapidly, while CO conversion begins to decline and can even reach negative values. This behaviour is a crucial point of interest and indicates a shift in the dominant reactions occurring in the system as the temperature increases.

The findings of Gao et al. [27] align with the current study's results, showing similar trends in the conversion of CO and CO_2 in the presence of stoichiometric hydrogen. These trends can be explained by the occurrence of the water–gas shift reaction, where carbon dioxide is consumed to produce carbon monoxide. CO conversion increases with increasing pressure across all temperature conditions. However, the trend for carbon dioxide conversion is non-monotonic. At low temperatures (below 650 °C), an increase in pressure leads to higher CO_2 conversion. In contrast, at higher temperatures (above 750 °C), increasing pressure reduces the overall conversion of carbon dioxide.

Additionally, it is noted that the impact of pressure on both CO and CO_2 conversion diminishes as pressure reaches higher values, typically above 8 bar. Beyond this point, further increases in pressure have limited effects on the conversion of carbon oxides. In contrast to the H_2-lacking scenario, if stoichiometric hydrogen is present in the gas mixture, discrete carbon dioxide conversion can be achieved if the reactor temperature is properly managed.

Fig. 7b and Fig. 8b illustrate the conversion of carbon monoxide and carbon dioxide with hydrogen content as a parameter, with pressure kept at the constant value of 1 bar.

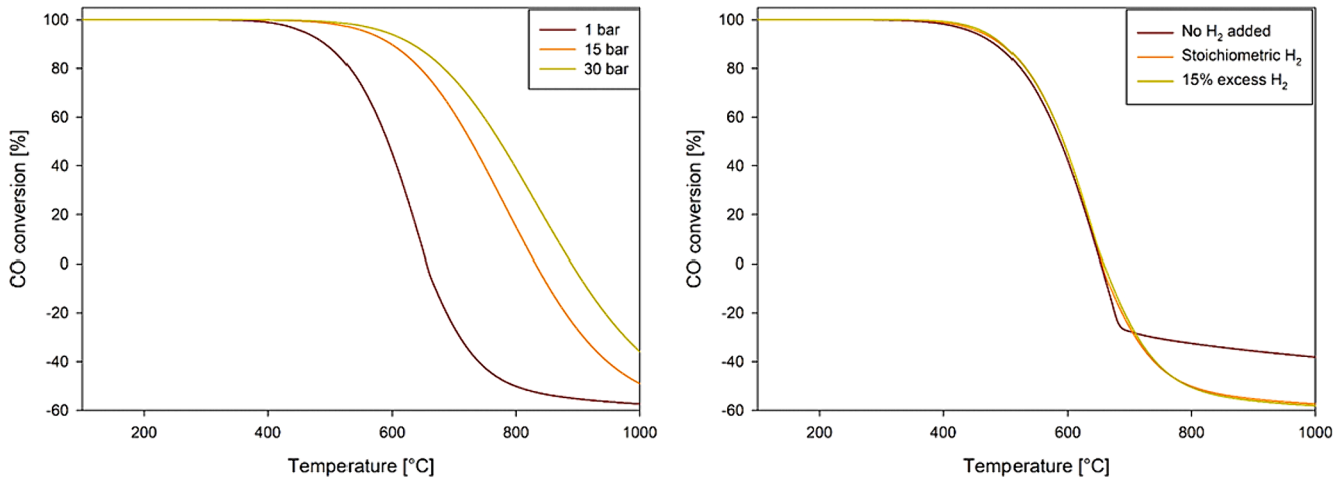

Fig. 7. Effect of pressure (a) and H_2 content (b) on CO conversion.

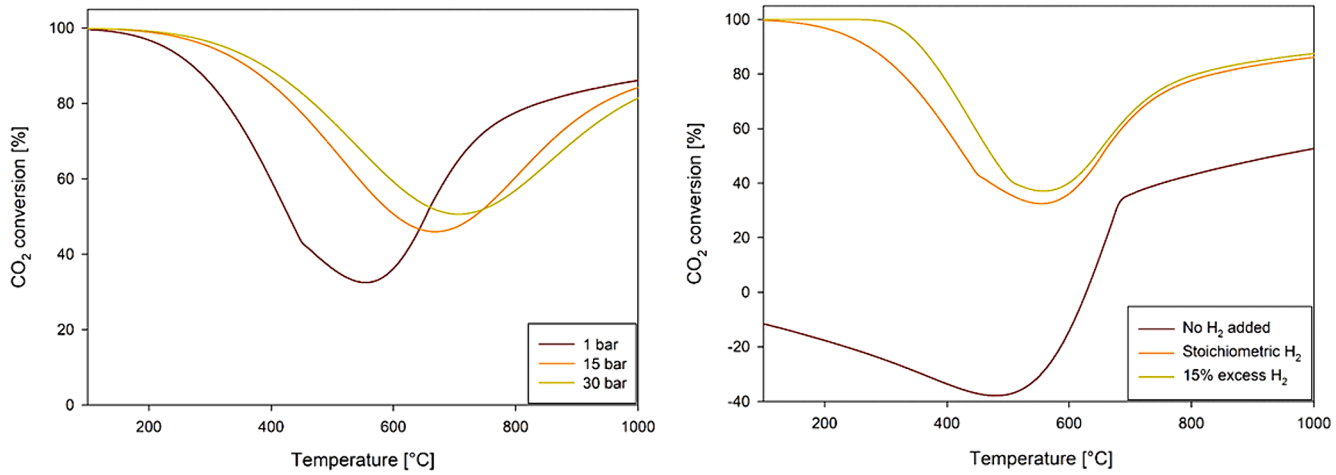

Fig. 8. Effect of pressure (a) and H_2 content (b) on CO_2 conversion.

The results show that while the hydrogen concentration has no significant influence on CO conversion, especially at temperatures below 700 °C, it has a substantial impact on CO_2 conversion. If no more hydrogen is supplied to the system, as previously discussed, carbon dioxide is produced if the temperature is less than 620 °C. Under stoichiometric condition, however, CO_2 conversion is always positive, with a minimum value of 32.5 %.

Fig. 8b also indicates that with a hydrogen surplus of 15 %, CO_2 conversion can be slightly further improved, reaching a minimum value of 37.1 %. However, despite this potential improvement, it should be noted that working with excess hydrogen is not currently seen as a viable solution due to stringent regulations for the quality of synthetic natural gas (SNG) that can be injected into the grid [14,28].

Similar conclusions can be drawn about the trends in methane yield and the solid carbon yield. Methane yield decreases with temperature and increases with pressure. Solid carbon formation is limited to a specific temperature range if stoichiometric hydrogen is available in the reacting mixture. A more detailed discussion about the thermodynamic trends of methane and solid carbon yields can be found in the Supplementary Material (cfr. Fig. S6 and Fig. S7). As expected, the addition of hydrogen during the methanation process leads to a synthetic natural gas (SNG) with higher calorific values compared to the original raw syngas and to the syngas-hydrogen mixture, as illustrated in Table 6:

3.2. Model validation results

The validation results based on the work of Khorsand et al. (2007) [20] are illustrated in Table 7:

The first column includes the input industry data at the reactor inlet used in the simulation. The second, third and fourth column show the outlet industrial data, the results obtained from the simulation of Khorsand et al. [20], and the outcomes from the current simulation. Upon comparison, it is evident that there is good agreement with the industry data and with Khorsand's results. The relative errors between the simulation results and actual industrial data are calculated to be less than 5 %, which indicates that the chosen kinetic model is appropriate to describe the behaviour of the system. The deviation in the temperature value can be ascribed to the hypothesis of perfect adiabatic conditions, which is not reached in real industrial reactors.

Table 6
Calorific values of raw syngas and SNG on a dry basis.

Calorific values of raw syngas and SNG on a dry-basis (MJ/Nm^3) STP 0 °C, 1 atm.		
	LHV	HHV
Raw syngas	3.72	4.00
Syngas-H_2 mixture	6.62	7.59
Equilibrium SNG	9.73	10.87

Table 7
Validation results based on ref. [20].

	INLET	OUTLET			Relative error [%]
	Input industrial data	Ref. [20]	Industrial data	This work	
CO [kmol h^{-1}]	20.5	0	0	0	0
CO_2 [kmol h^{-1}]	3.4	0	0	0	0
H_2 [kmol h^{-1}]	4186.7	4407.53	4111.5	4111.6	0
CH_4 [kmol h^{-1}]	26.1	55.61	50.1	50.0	0.2
H_2O [kmol h^{-1}]	58	92.12	85.3	85.3	0
Inert N_2 [kmol h^{-1}]	16.6	16.6	16.6	16.6	0
Temperature [K]	577.8	598	589	617.6	4.8
Pressure [bar]	29.4	29.38	29.2	29.39	0.6

3.3. Plant configuration results

The exit temperature of the reactor in system S1 is calculated to be 647 °C, which is considerably higher than the catalyst deactivation temperature attributed to sintering, as referenced in [8]. This observation is consistent with similar findings reported in the literature [10]. As the single methanation reactor cannot achieve complete conversion of all CO and CO_2 present in the syngas, the attained methane yield is not notably high, as shown in Table 8. The issue of catalyst sintering poses a significant challenge to the practicality of this technique.

From a technical perspective, it is imperative to implement temperature reduction measures to prevent catalyst deactivation. Additionally, reducing the temperature is also thermodynamically advantageous, as the methanation reactions are exothermic. In systems S2, S3 and S4, for the purpose of this work, the following definition of the recycle ratio is adopted (Eq. (6)):

$$R = \frac{mole\ flow\ rate\ of\ recycle}{mole\ flow\ rate\ of\ outlet\ stream} = \frac{N_R}{N_{OUT}} \quad (6)$$

The ideal recycling ratio for a fixed load, which is the volumetric gas flow rate to be treated, is the one that precisely attain equilibrium conditions at the reactor exit [10]. The recycle ratio is usually modulated in the range 0.5–3 [9]. In the present study, the recycle ratio was adjusted to achieve a desired outlet temperature of 550 °C, which was chosen as a constraint value for the system. By varying the catalyst bed length, equilibrium conditions were achieved at the reactor exit, ensuring the desired outlet temperature was met consistently. Fig. 9 depicts the temperature profile within a single fixed-bed reactor with (system S2) and without a recycling loop (system S1). The temperature in the recycle reactor rises progressively from the inlet temperature of 330 °C to the final constrained value of 550 °C, demonstrating the controlled temperature change that occurs within the reactor due to the recycling loop's influence.

Fig. 10 illustrates the critical behavior observed in the recycling ratio and its effect on reactor operation, particularly when the reactor's diameter is smaller than 17 cm. This phenomenon can be explained by examining the relationship between gas velocity, mean residence time, and reaction rates.

Table 8
Global performance of the methanation systems addressed in this work.

	S1	S2	S3	S4
CO conversion [%]	29.7	79.9	99.8	99.7
CO_2 conversion [%]	38.6	27.4	77.9	90.8
CH_4 yield [%]	36.1	62.6	92.1	96.6

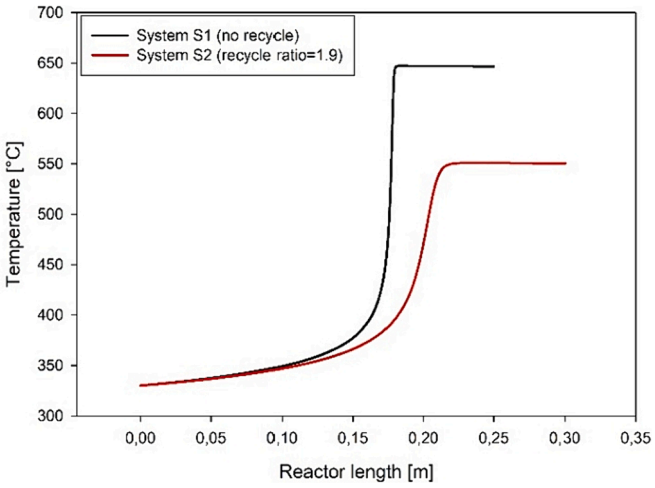

Fig. 9. Axial temperature profile in a FBR with and without recycle.

As the reactor's diameter decreases, the average gas velocity within the reactor increases, and the mean residence time of the gas decreases significantly, even at the same recycling ratio. When the residence time becomes too short, the reaction cannot proceed to the desired extent, leading to inadequate conversion of carbon oxides and potential reactor shutdown.

The critical value of the recycling ratio is the threshold beyond which the mean residence time becomes too short to facilitate the desired reaction. This critical value tends to increase with larger tube diameters. However, selecting a reactor with a diameter of 20 cm ensures that the critical value falls outside the range of the typical operating recycling ratios, thus safeguarding the reactor's smooth functioning.

The reactor diameter was set to 20 cm, and the recycled flow rate was adjusted to 117 kg h^{-1}, resulting in a molar-based recycle ratio of 1.9. Note that a 15 cm diameter proves to be suitable for the subsequent adiabatic reactors. As confirmed in Table 8, the recycling process has a beneficial impact on reactor performance since the mean temperature of the reaction is lower [12].

It should be noted that the indicators are calculated based on the streams that enter and exit the recycling loop. With the recycling process in place, the degree of carbon monoxide conversion increased significantly from 29.7 % to 79.9 %. Conversely, carbon dioxide conversion slightly decreased from 38.6 % to 27.4 %. However, the most notable improvement was observed in the methane yield, which increased from 36.1 % to 62.6 %.

System S3 achieves nearly complete carbon monoxide conversion and a considerable CO_2 conversion with a methane yield higher than 90 %. The total catalyst mass required to conduct the operation was calculated to be 59.4 kg.

For the System S4, the total catalyst mass required was calculated to be 41.9 kg, with a reduction of 40.5 % with respect to ystem S3 layout. It should be highlighted that system S4 achieves a higher conversion of CO_2 thanks to the condensers.

3.4. Sensitivity analysis & system optimization

3.4.1. Effect of plant pressure

In Fig. 11 (refer to Table S4 for data), the histograms demonstrate the impact of pressure on the catalyst mass required for the methanation system. The analysis is conducted while keeping all other parameters unchanged, except for the pressure. The data is presented for both the 5-stage system (including the last reactor) and the equivalent 4-stage system (excluding the last reactor). The comparison between the 5-stage and 4-stage systems indicates that the performance improvement achieved by adding the last reactor is relatively small, but it comes at the

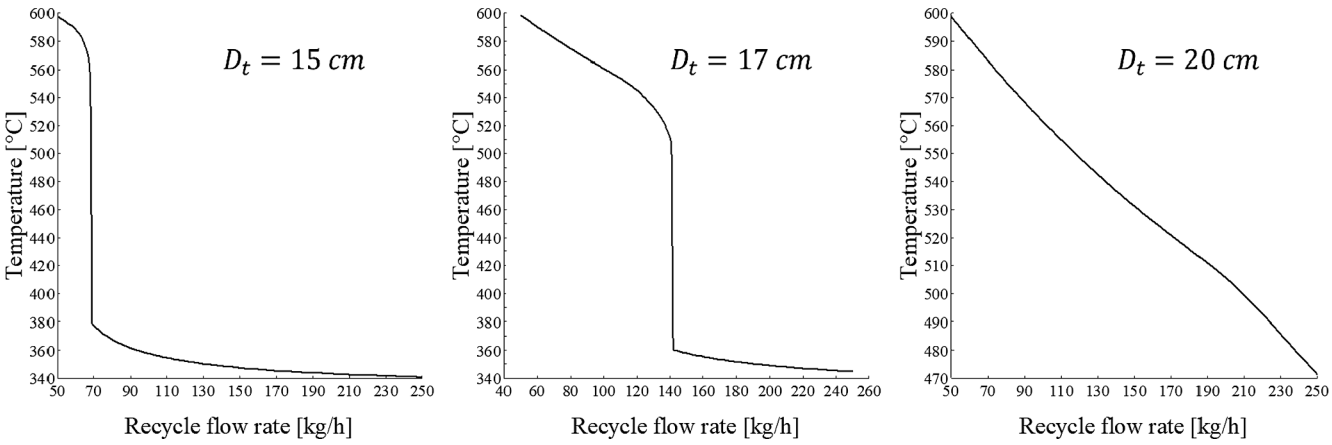

Fig. 10. Effect of the recycle ratio on the RFBR outlet temperature at different reactor diameters.

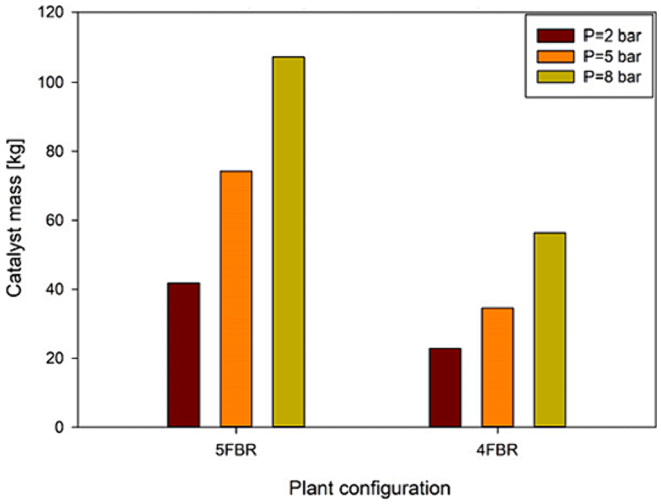

Fig. 11. Effect of plant pressure on catalyst mass required for operation.

cost of significantly higher catalyst mass consumption. This suggests that while the 5-stage system may slightly improve overall performance, it may not be the most economical option due to the additional catalyst requirement in the last reactor.

A higher catalyst mass is necessary to reach equilibrium conditions as plant pressure increases. This happens due to the higher flow velocity, which reduces the mean residence time of the gas in the reactor, making it necessary to use a longer catalyst bed to reach the equilibrium conditions. The analysis indicates that the catalyst mass needed for the 5-stage system increases significantly with higher operating pressures. For example, at 2 bar, the catalyst mass is 41.8 kg, but it rises to 107.3 kg at 8 bar. On the other hand, if the last reactor is excluded from the system (i.e., considering a 4-stage system instead of a 5-stage system), the catalyst mass at 2 bar is reduced to 22.8 kg, and at 8 bar, to 56.4 kg. This proves that the last reactor in the 5-stage system contributes significantly to the overall catalyst mass required for the process.

The provided figures, Fig. 12a, Fig. 12b, and Fig. 12c (refer to Table S5 for data), demonstrate the influence of pressure on carbon monoxide (CO) and carbon dioxide (CO_2) conversion, as well as on methane yield, in each reactor of the series. The figures show the results for three different operating pressures: 2 bar, 5 bar, and 8 bar. From Fig. 12a, it can be observed that increasing the pressure from 2 bar to 5 bar leads to a favorable effect on CO conversion. At 2 bar, the CO conversion reaches 79.9 % in the RFBR, but at 5 bar, it significantly increases to approximately 90.1 %. This demonstrates that higher pressure enhances CO conversion, making it a beneficial factor to achieve higher conversion levels in the reactors. Similarly, from the data in Fig. 12b, it is clear that increasing the pressure from 2 bar to 5 bar also has a positive effect on CO_2 conversion. At 2 bar, the CO_2 conversion is around 27.4 %, which rises to approximately 40.4 % at 5 bar.

Fig. 12c shows the methane yield in each reactor of the series at the different pressures. The data shows that increasing the pressure from 2 bar to 5 bar results in a considerable increase in methane yield. At 2 bar, the methane yield is approximately 62.6 %, and at 5 bar, it rises to around 72.3 %. On the other hand, going from 5 bar to 8 bar seems to have a minor effect on performance.

Based on the results obtained from the simulations, a pressure value of 5 bar was selected for the final system. This pressure value was chosen because it is the lowest pressure that limits solid carbon deposition (cfr. Fig. S7 in the Supplementary Material), which is a critical factor to ensure the efficient and stable operation of the methanation reactors.

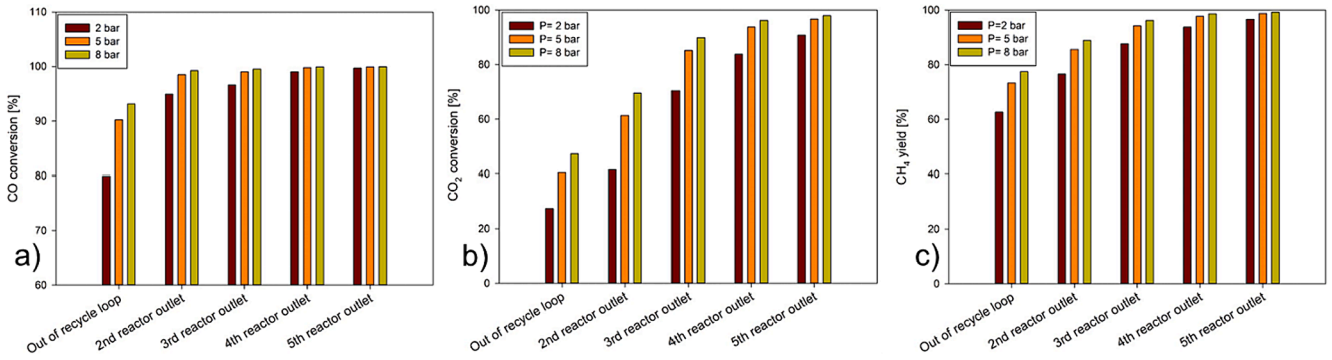

Fig. 12. Effect of plant pressure on CO conversion (a), CO_2 conversion (b) and CH_4 yield (c).

While higher pressures might slightly improve the overall performance of the system, they also come with increased capital costs and safety considerations. For small-scale methanation facilities, such as those addressed in this work, it is essential to find a balance between achieving high conversion and yield while keeping costs reasonable. It is worth noting that even using a 4-stage system with an operating pressure of 5 bar would result in good overall performance. The differences in conversion and yield between the 4-stage and 5-stage systems are relatively small, indicating that adding an additional reactor does not provide significant gains in performance. For example, switching from a 5-stage system to a 4-stage system with a fixed pressure of 5 bar would only result in a decrease of 0.12 % in CO conversion, a decrease from 96.7 % to 93.7 % in CO_2 conversion, and a 1.1 % drop in overall methane yield.

3.4.2. Effect of reactor inlet temperature

In the simulations conducted to investigate the effect of increasing the inlet gas temperature from 330 °C to 350 °C, the plant pressure was set to 5 bar, and the outlet temperature of the RFBR (Recycling Fixed-Bed Reactor) was maintained at 550 °C, resulting in a fixed recycle ratio.

Fig. 13 (refer to Table S6 for data) demonstrate that raising the inlet temperatures is indeed advantageous as it leads to lower catalyst expenses. The increase in gas temperature entering the fixed bed reactor enhances the reaction rate, resulting in a reduced overall catalyst mass required for the system to reach the equilibrium conditions at the reactor outlet.

In the 4-stage system, when the inlet gas temperature is increased to 350 °C, the overall catalyst bed length is reduced from 1.9 m to 0.95 m and the catalyst mass is reduced from 34.5 kg to 17.6 kg. These substantial reductions in catalyst requirements offer both cost-saving benefits and improved efficiency in catalyst replacement, as aged and deactivated catalysts need to be replaced regularly.

Fig. 14a and Fig. 14b (refer to Table S7 for data) illustrate how increasing the inlet temperature affects the reactor's performance. Interestingly, the reduction in both CO and CO_2 conversion is almost negligible. For CO conversion, the decrease is less than 1 %, and for CO_2 conversion, it ranges from 1 % to 3 %. This shows that the negative impact of the increased inlet temperature on conversion efficiency is minimal.

On the other hand, the cost savings associated with the corresponding reduction in catalyst requirements significantly outweigh the minor decrease in conversion. By setting the inlet temperatures of all reactors to 350 °C, the overall catalyst expenses are reduced, leading to a more cost-effective operation.

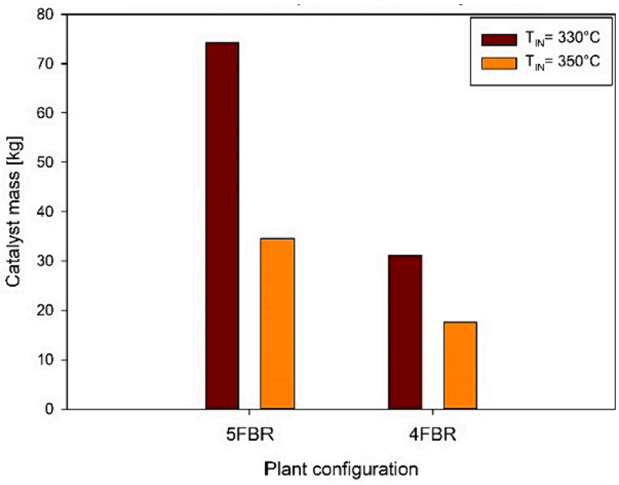

Fig. 13. Effect of reactor inlet temperature on the total catalyst mass.

3.4.3. Effect of the RFBR's outlet temperature (i.e., recycle Ratio)

As previously mentioned, increasing the recycling ratio in exothermic processes can indeed lower the reactor mean temperature, which may have potential benefits in terms of performance. To investigate this further, simulations were conducted with the pressure set to 5 bar, reactor inlet temperatures set to 330 °C, and considering the presence of three condensers.

The outlet temperature of the first reactor was chosen as the indicator to compare two scenarios. By adjusting the recycling ratio, the outlet temperature of the first reactor can be controlled, which subsequently influences the mean temperature in the reactor system.

Fig. 15 (refer to Table S8 for data) shows the relationship between the outlet reactor temperature (thus, the recycle ratio) and the catalyst mass required in the system. When the outlet reactor temperature is decreased (corresponding to an increase in the recycle ratio), it leads to a decrease in the reaction rate due to feed gas dilution, resulting in a need for a higher catalyst mass to achieve the desired conversion. For instance, in a 4-stage system operating with an outlet temperature of 550 °C in the first reactor, it requires a total catalyst mass of 34.5 kg. However, if the outlet temperature is reduced to 500 °C by increasing the recycle ratio, the system would need a longer catalyst bed and a total catalyst mass of 53.9 kg (+56.2 %).

As depicted in Fig. 16a and 16b (refer to Table S9 for data), increasing the recycle ratio has a more pronounced impact on the performance of the first reactor (RFBR). This leads to a notable improvement in CO and CO_2 conversion rates in the RFBR. Specifically, when the recycle ratio is increased, the overall reactor temperature decreases, which favors exothermic reactions and improves the thermodynamic conditions for CO and CO_2 conversion. As a result, the CO conversion increases from 90.17 % to 96.35 %, and the CO_2 conversion increases from 40.38 % to 51.22 % in the RFBR.

However, as the gas stream moves through next reactors in the series, the impact of the higher recycle ratio becomes less significant on the overall performance. This is because the benefits of enhanced thermodynamic conditions are primarily concentrated in the first stages of the process.

While it is advantageous to optimize the performance of the first reactor, lowering the output temperature to 500 °C in the last reactor may not be as beneficial. The overall methane concentration at the fourth stage is still the same, and the advantages gained from further reducing the output temperature become less significant. Moreover, the associated increase in compression costs and catalyst mass may not justify the marginal performance improvement obtained.

3.4.4. Effect of condenser location

Placing a water removal unit after each reactor would be more costly compared to having a single condenser in an optimized location. To determine the best location, different layouts for the condenser were simulated, specifically after the second, third, and fourth reactors in the flowsheet. Because it has no effect on reaction rate or equilibrium conditions in any reactor, placing the condenser after the fourth reactor in a four-stage system is equal to having no water removal at all.

Fig. 17 (refer to Table S10 for data) presents a bar chart showing the catalyst mass required for a 5-stage system and for a 4-stage system. Based on the results, the most cost-effective configuration is the one with the water removal condenser placed after the third reactor. In this configuration, the total catalyst mass required for the 4-stage system is 37.7 kg. If the water removal condenser is located after the second fixed-bed reactor, the catalyst mass increases to 40.1 kg (+6.3 %). However, if no water removal is performed in the system, the catalyst mass required increases significantly to 56.8 kg (+50.6 %). These findings align with those reported in the literature [12], further supporting the conclusion that placing the water removal condenser after the third reactor is the most cost-effective and efficient configuration.

Fig. 18 illustrates the effect of the condenser's location on the global CO conversion, CO_2 conversion and methane yield within the 4-stage

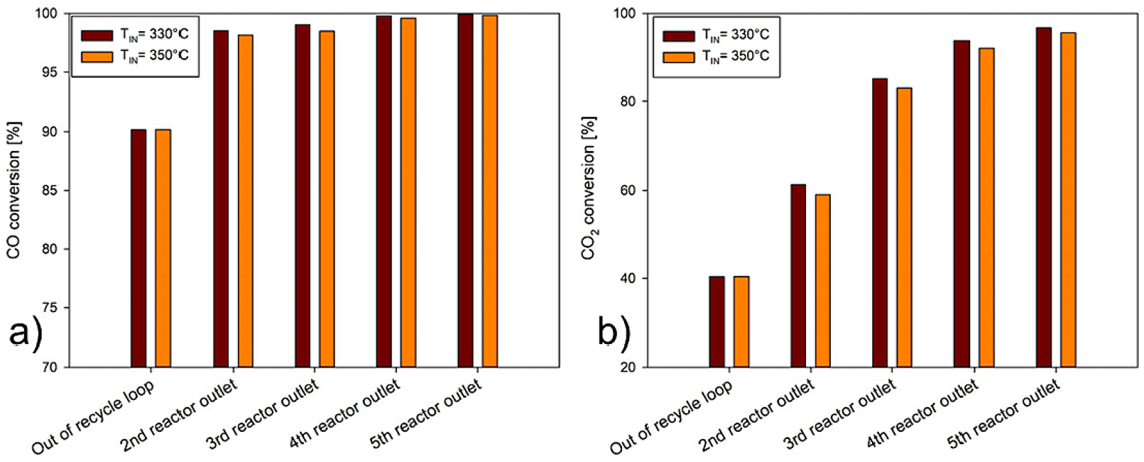

Fig. 14. Effect of reactor inlet temperature on CO (a) and CO_2 (b) conversion.

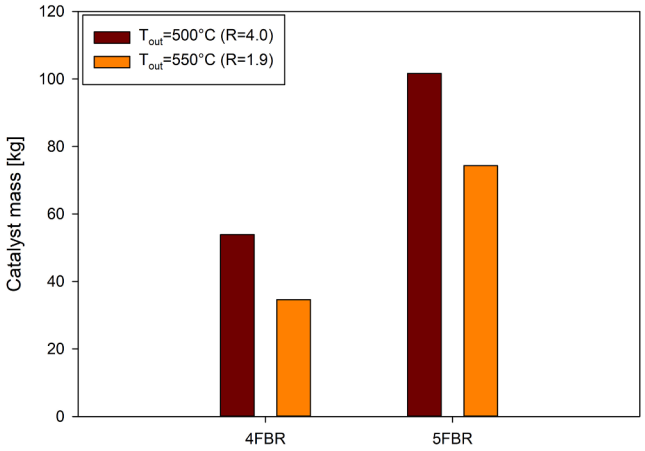

Fig. 15. Effect of RFBR's outlet temperature on the total catalyst mass required.

system (refer to Table S11 for data). The results show that when the condenser is placed after the third reactor, CO_2 conversion is still over 90 %. Furthermore, with the presence of the condenser, CO_2 conversion increases from 84.2 % to 91.5 %. This significant improvement in CO_2 conversion demonstrates the importance of effective water removal in enhancing the overall performance of the methanation process.

3.5. Optimized system

Fig. 19 depicts the optimized Aspen Plus simulation flowsheet for the methanation system based on the analysis performed. The optimized system consists of four fixed-bed reactors, with an inlet temperature of 350 °C, operating at a pressure of 5 bar. The outlet temperature of the recycle fixed-bed reactor is set to 550 °C. A single condenser is

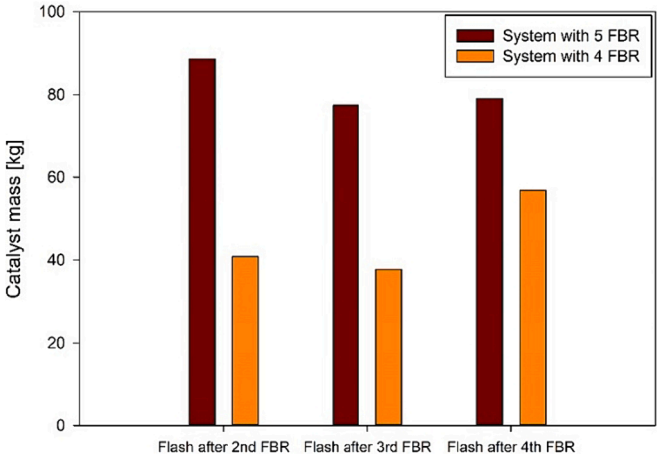

Fig. 17. Effect of condenser location on catalyst mass required.

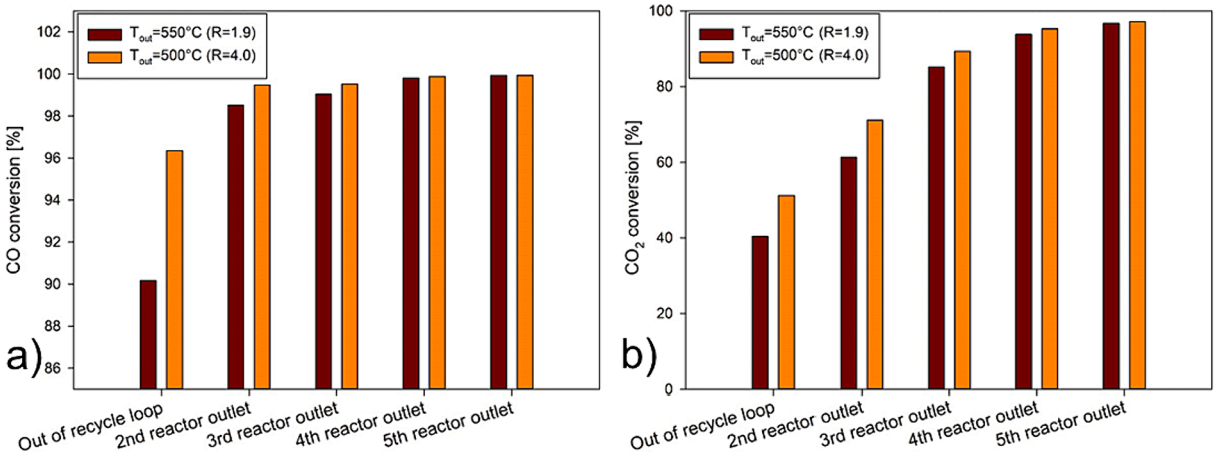

Fig. 16. Effect of RFBF's outlet temperature on CO (a) and CO_2 (b) conversion.

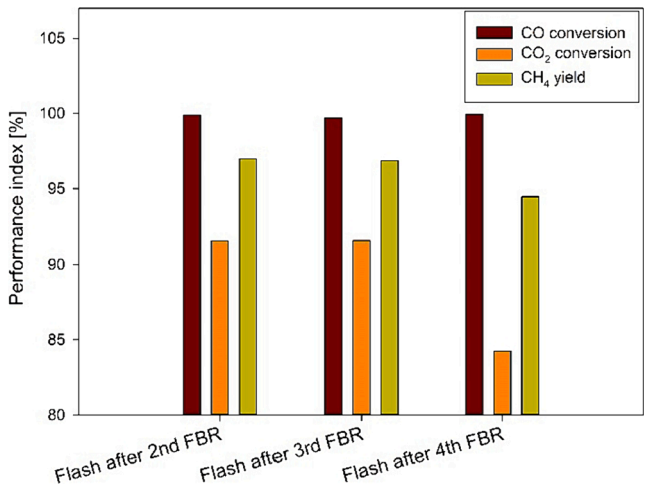

Fig. 18. Effect of condenser location on the overall CO and CO_2 conversion, and methane yield. (4-stage system).

strategically placed after the third adiabatic stage for efficient water removal. The condenser was operated at 30 °C and 5 bar, obtaining a water removal efficiency of 97.5 %.

The simulation results highlight the significant role of the first reactor with a recycle loop in the methanation system. It is responsible for a substantial portion of the carbon monoxide conversion (90 %) and a significant fraction of carbon dioxide conversion (about 40 %).

As the syngas passes through the next reactors, CO_2 conversion occurs at a slower rate and requires more reaction steps to reach higher levels of conversion. However, with the four-reactor system, the system achieves a carbon monoxide conversion of 99.4 % and a carbon dioxide conversion of 89.3 %, resulting in an overall methane yield of 95.9 %. The total catalyst mass required for the operation was calculated to be 20 kg. Details about the conversion achieved in each reactor of the series and about the design characteristics of each FBR are available in the Supporting Material (Table S3, Fig. S8).

Fig. 20 presents a comprehensive representation of the final system determined in this study. The chart illustrates the changes in methane concentration as a function of temperature, providing a clear visualization of the steps leading from the low-quality syngas to synthetic natural gas (SNG). The dashed lines on the chart represent the equilibrium curves of methane content, calculated using the Aspen Plus software through the Gibbs energy minimization method. Two equilibrium curves are shown: one for the fed syngas and another for the gas mixture that enters the final reactor. This distinction is essential because water removal alters the equilibrium composition of the produced gas. The chart also includes various lines to represent different components of the system. Horizontal lines indicate coolers, which are responsible for reducing the temperature of the gas stream. Oblique lines represent adiabatic reactors, where the chemical reactions take place. The vertical line represents the isothermal water removal process, which increases the methane content without involving any chemical reactions. As a consequence of the design procedure, thermodynamic equilibrium conditions are met at the outlet of each reactor.

3.5.1. Calorific values

The calorific value is a crucial parameter in defining the quality of the syngas, as it indicates the energy content and potential combustion properties of the gas for energy applications. The syngas produced with the optimized system of Fig. 19 has the following molar composition: 64.35 % N_2, 4.39 % H_2, 3.74 % H_2O, 26.4 % CH_4, 1 % CO_2, 0.12 % CO. In the context of the optimized flowsheet depicted in Fig. 19, the calorific values were calculated for each reactor outlet stream using the Aspen Plus analysis tool. The calculations were performed at standard temperature and pressure (STP, 0 °C and 1 atm) conditions to facilitate comparisons. The benefit of converting the syngas to synthetic natural gas (SNG) is clarified by the examination of Fig. 21, which shows the calorific values on a volume basis (refer to Table S12 for data). The final SNG obtained in the optimized system exhibits a calorific value of 8.6 MJ/Nm^3, which is substantially higher than the calorific value of the raw syngas before hydrogen addition (3.16 MJ/Nm^3) but lower than the equilibrium value reported in Table 6. Specifically, the hydrogen addition -from surplus renewable energy sources and thus free of charge - results in a remarkable 78 % increase in the calorific value compared to the raw syngas. The first reactor leads to a 130 % increase, followed by 148 % for the second reactor, 160 % for the third reactor, and a 173 % increase in the calorific value at the last reactor. Higher heating values may be obtained if a low N_2-content syngas from biomass gasification is used as the raw feedstock of the process.

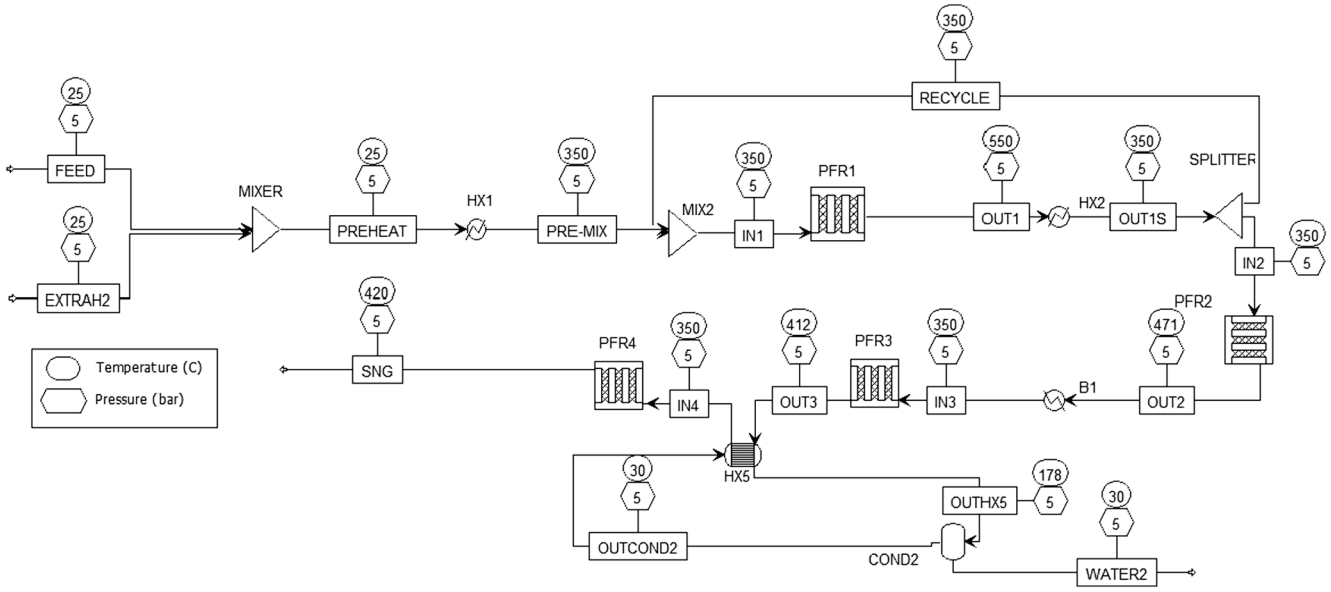

Fig. 19. Aspen Plus flowsheet for the final system.

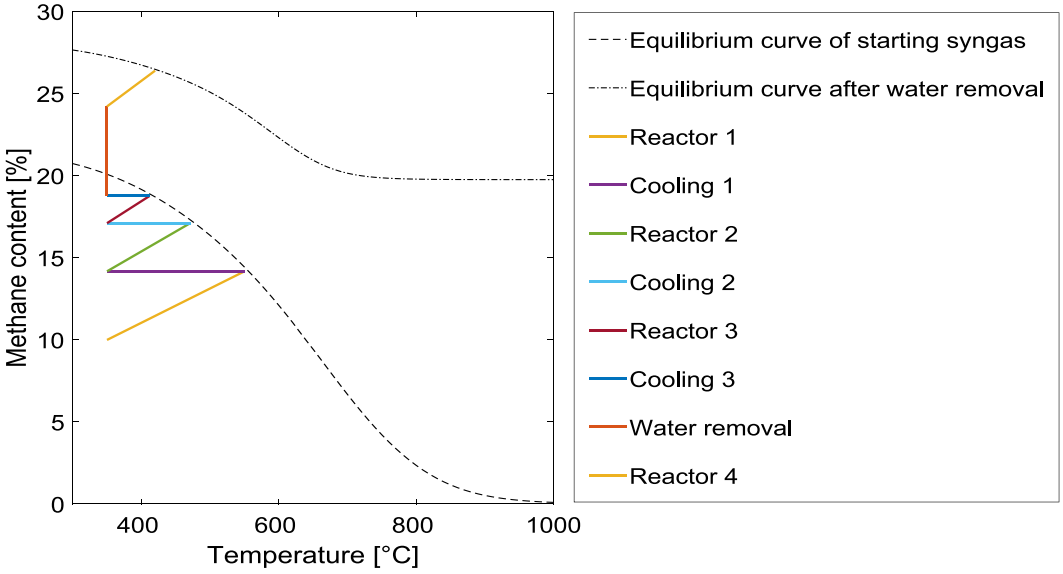

Fig. 20. Optimal system: Methane content [%] vs Temperature [°C] chart.

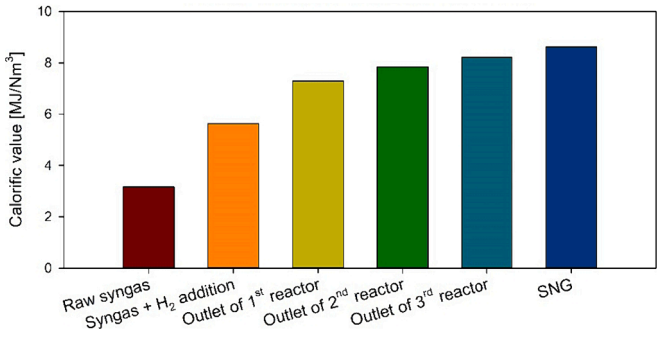

Fig. 21. Calorific values of the gas streams on a volume basis (STP conditions).

3.5.2. *Carbon deposition*

As stated in the kinetic model description (cf. Section 2.2 Kinetic model), the rate of the solid carbon production was not modelled in this study. Attempts of finding an appropriate and valid kinetic expression for carbon deposition go back to 1980s [29] and 1990s [30]. In the present study, a simple thermodynamic analysis was adopted to determine the operating conditions that would prevent or minimize carbon deposition in the methanation system being investigated. It was useful to check if carbon deposition is avoided in the system of Fig. 19. For this purpose, the incoming gas to each reactor was fed into an RGIBBS block within Aspen Plus, allowing the determination of the equilibrium product distribution and the computation of the carbon yield. The resulting carbon yield curve for the reactors is presented in Fig. 22. The black curve refers to reactors 1, 2, and 3, while the blue curve corresponds to the last reactor. The distinction between these curves is necessary due to the water removal stage following the third fixed-bed reactor, which alters the equilibrium composition. It is observed that the first three reactors are characterized by a bell-shaped carbon yield curve, indicating that carbon deposition is limited within a specific temperature range. In contrast, the last reactor shows a monotonic and increasing trend in carbon yield. This behavior is attributed to the lower water content in the last reactor, which enables higher carbon deposition.

According to the findings, the first three reactors effectively prevent any carbon deposition as the carbon yield is zero throughout the operating temperature range of 350–550 °C, indicating that the conditions in these reactors do not favor solid carbon formation. However, the analysis also reveals that the last reactor, which operates between 350 and 420 °C, can reach a carbon yield of 12 %. This means that some carbon

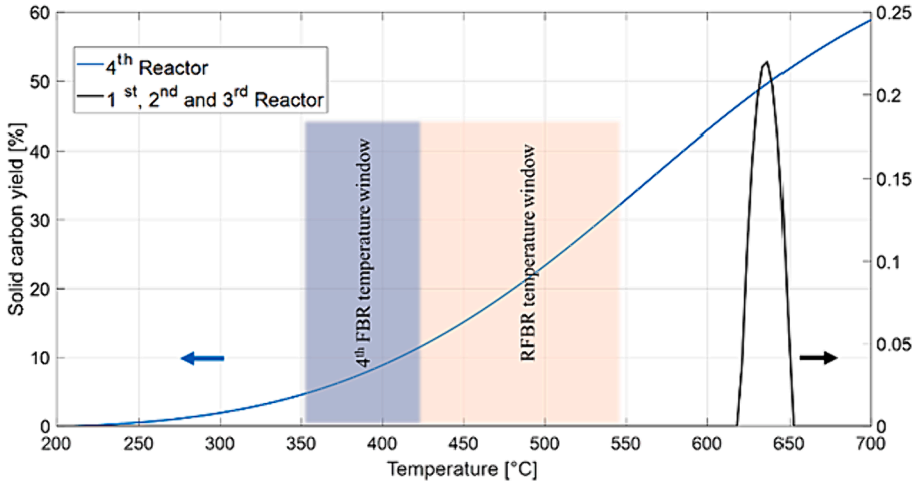

Fig. 22. Solid carbon deposition: a thermodynamic assessment in the optimized system.

deposition is possible in this reactor, and caution should be exercised to prevent excessive carbon formation, which could lead to catalyst deactivation and reduced reactor performance. As reported in the open literature, steam addition to the syngas is a common strategy to limit carbon deposition, therefore water removal seems to favour solid carbon formation [27,31].

The identification of potential improvement strategies to minimize carbon production and preserve catalyst life is crucial for the successful and efficient operation of the methanation system. The use of promoters in the nickel catalyst is one approach that can enhance the catalytic activity and selectivity, leading to improved carbon conversion and reduced carbon deposition. Partial steam removal can be another effective strategy to limit carbon deposition when operating with stoichiometric hydrogen content [27,31].

While the carbon deposition observed in the fourth reactor appears to be limited and may not have a substantial impact on reactor performance in the context of this study, it is essential to exercise caution and consider additional precautions during the real design phase. A more detailed and comprehensive analysis of carbon deposition, including kinetic modeling and pilot-scale experiments, is necessary to fully understand the behavior of the system and ensure its best performance in practical applications.

4. Conclusions

The present research aims to investigate the theoretical feasibility of the methanation process to upgrade a low-quality syngas coming from small-scale air gasification of biomass, to date poorly investigated in the pertinent literature. The performed thermodynamic analysis allowed to understand the effect of temperature, pressure, and hydrogen concentration on the performance of the methanation process in nitrogen-diluted conditions. Results showed that, as expected, the process requires at least stoichiometric hydrogen for complete methanation of both CO and CO_2. Additionally, although low temperatures (300–550 °C) and high pressures are favourable to the methanation process – leading to high methane yield and negligible solid carbon deposition, pressure values above 8 bar do not significantly improve the process performance.

The kinetic investigation included the design and simulation of different methanation system configurations. The parameter-by-parameter sensitivity study demonstrated that higher plant pressure and higher inlet temperature at each fixed bed reactor increase the global conversion of both CO and CO_2. On the other hand, increasing the recycle ratio at the first reactor is not convenient as it does not modify the final composition of the SNG produced. The presence of a condenser after the third adiabatic stage proved to increase the overall CO_2 methanation as reported in previous literature investigations.

In conclusion, the upgrading of nitrogen-diluted syngas via catalytic methanation at small scale poses some major challenges. Results show that the produced SNG is not suitable for direct grid injection but can be used for small-scale applications and to store surplus renewable energy into a manageable and safe energy carrier.

Funding

The Authors thank the iENTRANCE@ENL: Infrastructure for Energy TRAnsition aNd Circular Economy @ EuroNanoLab Project (Award Number: 128 dated 21/06/2022 – Project Code: IR0000027 -) funded under the National Recovery and Resilience Plan (NRRP), Mission 04 Component 2 Investment 3.1 – NextGenerationEU, Call for tender n. 3264 dated 28/12/2021 for supporting the PhD grant of Biagio Ciccone.

CRediT authorship contribution statement

Biagio Ciccone: Writing – original draft, Visualization, Investigation, Data curation. **Fabio Murena:** Writing – review & editing, Supervision, Methodology, Conceptualization. **Giovanna Ruoppolo:** Writing – review & editing, Supervision, Methodology. **Massimo Urciuolo:** Writing – review & editing, Supervision, Methodology. **Paola Brachi:** Writing – review & editing, Supervision, Methodology, Investigation, Conceptualization.

Declaration of competing interest

The authors declare that they have no known competing financial interests or personal relationships that could have appeared to influence the work reported in this paper.

Data availability

No data was used for the research described in the article.

Appendix A. Supplementary data

Supplementary data to this article can be found online at https://doi.org/10.1016/j.applthermaleng.2024.122901.

References

[1] K. Zaman, M.A. Moemen, Energy consumption, carbon dioxide emissions and economic development: evaluating alternative and plausible environmental hypothesis for sustainable growth, Renew. Sust. Energ. Rev. 74 (2017) 1119–1130, https://doi.org/10.1016/j.rser.2017.02.072.
[2] N. Patel, Environmental and economical effects of fossil fuels, J. Recent Res. Eng. Tech. 1 (2014) 1–12.
[3] P.T. Brown, K. Caldeira, Greater future global warming inferred from earth's recent energy budget, Nature 552 (7683) (2017) 45–50, https://doi.org/10.1038/nature24672.
[4] P. McKendry, Energy production from biomass (part 1): overview of biomass, Bioresour. Technol. 83 (1) (2002) 37–46, https://doi.org/10.1016/S0960-8524(01)00118-3.
[5] F. Patuzzi, D. Basso, S. Vakalis, D. Antolini, S. Piazzi, V. Benedetti, E. Cordioli, M. Baratieri, State-of-the-art of small-scale biomass gasification systems: an extensive and unique monitoring review, Energy 223 (2021) 120039, https://doi.org/10.1016/j.energy.2021.120039.
[6] Y.A. Situmorang, Z. Zhao, A. Yoshida, A. Abudula, G. Guan, Small-scale biomass gasification systems for power generation (< 200 kW class): a review, Renew. Sust. Energ. Rev. 117 (2020) 109486.
[7] H. Yang, C. Zhang, P. Gao, H. Wang, X. Li, L. Zhong, W. Wei, Y. Sun, A review of the catalytic hydrogenation of carbon dioxide into value-added hydrocarbons, Catal. Sci. Technol. 7 (20) (2017) 4580–4598, https://doi.org/10.1039/C7CY01403A.
[8] S. Rönsch, J. Schneider, S. Matthischke, M. Schlüter, M. Götz, J. Lefebvre, P. Prabhakaran, S. Bajohr, Review on methanation–from fundamentals to current projects, Fuel 166 (2016) 276–296, https://doi.org/10.1016/j.fuel.2015.10.111.
[9] H. Er-Rbib, C. Bouallou, Modeling and simulation of CO methanation process for renewable electricity storage, Energy 75 (2014) 81–88, https://doi.org/10.1016/j.energy.2014.05.115.
[10] S. Matthischke, S. Roensch, R. Güttel, Start-up time and load range for the methanation of carbon dioxide in a fixed-bed recycle reactor, Ind. Eng. Chem. Res. 57 (18) (2018) 6391–6400, https://doi.org/10.1021/acs.iecr.8b00755.
[11] R.Y. Chen, C.T. Yu, C.C. Wang, Numerical simulation on the effect of operating conditions and syngas compositions for synthetic natural gas production via methanation reaction, Fuel 185 (2016) 394–409, https://doi.org/10.1016/j.fuel.2016.07.123.
[12] Y.L. Kao, P.H. Lee, Y.T. Tseng, I.L. Chien, J.D. Ward, Design, control and comparison of fixed-bed methanation reactor systems for the production of substitute natural gas, J. Taiwan Inst. Chem. Eng. 45 (5) (2014) 2346–2357, https://doi.org/10.1016/j.jtice.2014.06.024.
[13] G. Song, J. Xiao, C. Yan, H. Gu, H. Zhao, Quality of gaseous biofuels: statistical assessment and guidance on production technologies, Renew. Sust. Energ. Rev. 169 (2022) 112959, https://doi.org/10.1016/j.rser.2022.112959.
[14] J. Savickis, L. Zemite, N. Zeltins, I. Bode, L. Jansons, E. Dzelzitis, A. Koposovs, A. Selickis, A. Ansone, The biomethane injection into the natural gas networks: the EU'S gas synergy path, Latv. J. Phys. Tech. Sci 57 (4) (2020) 34–50, https://doi.org/10.2478/lpts-2020-0020.
[15] I. Kiendl, M. Klemm, A. Clemens, A. Herrman, Dilute gas methanation of synthesis gas from biomass gasification, Fuel 123 (2014) 211–217.
[16] D. Cirillo, M. Di Palma, M. La Villetta, A. Macaluso, A. Mauro, L. Vanoli, A novel biomass gasification micro-cogeneration plant: experimental and numerical analysis, Energy Convers. Manag. 243 (2021) 114349, https://doi.org/10.1016/j.enconman.2021.114349.
[17] C.H. Bartholomew, Mechanisms of catalyst deactivation, Appl. Catal A-Gen. 212 (1-2) (2001) 17–60, https://doi.org/10.1016/S0926-860X(00)00843-7.

[18] Aspen Physical Property System, Physical Property Methods and Models 11.1, 2001.
[19] J. Xu, G.F. Froment, Methane steam reforming, methanation and water-gas shift: I, Intrinsic Kinetics. Aiche J. 35 (1) (1989) 88–96, https://doi.org/10.1002/aic.690350109.
[20] K. Khorsand, M.A. Marvast, N. Pooladian, M. Kakavand, Modeling and simulation of methanation catalytic reactor in ammonia unit, Pet. Coal 49 (1) (2007) 46–53.
[21] T.J. Schildhauer, S.M.A. Biollaz (Eds.), Synthetic Natural Gas: from Coal, Dry Biomass, and Power-to-Gas Applications, John Wiley & Sons, 2016.
[22] D.R. Woods, Rules of thumb in engineering practice, John Wiley & Sons, 2007.
[23] D.W. Green, M.Z. Southard, Perry's chemical engineers' handbook, McGraw-Hill Education, 2019.
[24] Á. Pethö, R.D. Noble, Residence Time Distribution Theory in Chemical Engineering: Proceedings of a Summer School Held at Bad Honnef, August 15-25, 1982.
[25] T. Burger, P. Donaubauer, O. Hinrichsen, On the kinetics of the co-methanation of CO and CO_2 on a CO-precipitated ni-al catalyst, Appl. Catal. 282 (2021) 119408, https://doi.org/10.1016/j.apcatb.2020.119408.
[26] A. Kambolis, T.J. Schildhauer, O. Kröcher, CO methanation for synthetic natural gas production, Chimia (aarau). 69 (10) (2015) 608–613, https://doi.org/10.2533/chimia.2015.608.
[27] J. Gao, Y. Wang, Y. Ping, D. Hu, G. Xu, F. Gu, F. Su, A thermodynamic analysis of methanation reactions of carbon oxides for the production of synthetic natural gas, RSC Adv. 2 (6) (2012) 2358–2368, https://doi.org/10.1039/C2RA00632D.
[28] UNI (Ente Nazionale Italiano di Unificazione). "UNI/TS 11537:2019 - [Immissione di biometano nelle reti di trasporto e distribuzione di gas naturale]," 2019.
[29] D.C. Gardner, C.H. Bartholomew, Kinetics of carbon deposition during methanation of carbon monoxide, Ind. Eng. Chem. Prod. Res. Dev. 20 (1) (1981) 80–87, https://doi.org/10.1021/i300001a007.
[30] M.C. Demicheli, E.N. Ponzi, O.A. Ferretti, A.A. Yeramian, Kinetics of carbon formation from CH4-H2 mixtures on nickel-alumina catalyst, J. Chem. Eng. 46 (3) (1991) 129–136, https://doi.org/10.1016/0300-9467(91)87004-T.
[31] F. Massa, A. Coppola, F. Scala, A thermodynamic study of sorption-enhanced CO_2 methanation at low pressure, J. CO_2 Util. 35 (2020) 176–184, https://doi.org/10.1016/j.jcou.2019.09.014.